

Space Group Symmetry of Chiral Fe-deficient van der Waals Magnet $\text{Fe}_{3-x}\text{GeTe}_2$ Probed by Convergent Beam Electron Diffraction

S. Subakti,^{1,*} D. Wolf,¹ O. Zaiets,^{1,2} S. Parkin,³ and A. Lubk^{1,2,4,†}

¹*Leibniz Institute for Solid State and Materials Research Dresden, Helmholtzstraße 20, 01069 Dresden, Germany*

²*Institute of Solid State and Materials Physics, TU Dresden, Haeckelstraße 3, 01069 Dresden, Germany*

³*Department for Nano-Systems from Ions, Spins, and Electrons (NISE),*

Max Planck Institute of Microstructure Physics, Weinberg 2, 06120 Halle(Saale), Germany

⁴*Würzburg–Dresden Cluster of Excellence ct.qmat, TU Dresden, 01062 Dresden, Germany*

Crystal structure symmetry of Fe-deficient $\text{Fe}_{2.9}\text{GeTe}_2$ at room temperature has been investigated by a combination of selected-area electron diffraction (SAED) and convergent-beam electron diffraction (CBED). By symmetry analysis of CBED patterns along different zone axis, the space group of $\text{Fe}_{2.9}\text{GeTe}_2$ at room-temperature has been identified as $P6_3mc$ (No.186), which derives from the high-symmetry parent system Fe_3GeTe_2 ($P6_3/mmc$) by breaking the mirror symmetry along the six-fold rotation axis. The $P3m1$ (No.156) space group previously reported for $\text{Fe}_{2.9}\text{GeTe}_2$ is a subgroup of $P6_3mc$ suggesting further possible symmetry breaks in this non-stoichiometric system.

I. INTRODUCTION

The two-dimensional (2D) van der Waals (vdWs) magnets with general formula $\text{Fe}_{n-x}\text{GeTe}_2$ ($n = 3, 4, 5$) have emerged not only as a promising platform for emergent unconventional physics, but also for technological applications in spintronics [1]. Among this family of compounds, the Fe-deficient $\text{Fe}_{3-x}\text{GeTe}_2$ system has attracted particular attention due to the presence of a metallic antiferromagnetic (AFM) state on a quasi-2D layered hexagonal lattice, where Fe_{3-x}Ge slabs are sandwiched between two vdWs bonded Te layers [2] (centrosymmetric space group $P6_3/mmc$ (No.194) at room temperature with unit cell parameters $a \sim 3.99 \text{ \AA}$, $c \sim 16.33 \text{ \AA}$ [3–6] Here, the quasi-2D nature in combination with sizeable spin-orbit coupling leads to strong magnetocrystalline anisotropy and a rather high Curie temperature ($T_c \sim 220 \text{ K}$) [7]. Consequently, deliberately engineering cation vacancies and cation element substitution in $\text{Fe}_{3-x}\text{GeTe}_2$ opens a way to tailor the magnetic properties [3].

The existence of Néel-type skyrmions in bulk $\text{Fe}_{3-x}\text{GeTe}_2$ [8] and their possible manipulation via electric current pulses predestines this material system as prominent building blocks for spintronic devices [9–11]. Here literature offers different mechanism for the existence of Néel-type skyrmions in this nominally centrosymmetric system. Xu et al. argue that specific forms of fourth-order interaction can stabilize skyrmions even in centrosymmetric $\text{Fe}_{3-x}\text{GeTe}_2$ [12]. A second possible mechanism is the breaking of inversion symmetry of the high-symmetry phase (point group $6/mmm$) to non-centrosymmetric point groups of type C_{6v} ($6mm$), C_{3v} ($3m$), or C_{2v} ($mm2$) allowing for a sizable antisymmetric exchange (Dzyaloshinskii-Moriya) interaction (DMI) [13] that favors Néel-type spin modulations. Indeed, Chakraborty et al. proposed the non-

centrosymmetric trigonal $P3m1$ (No.156) [8] space group (point group symmetry $3m$) as proper symmetry of $\text{Fe}_{2.9}\text{GeTe}_2$, by analyzing x-ray diffraction data. We note that this space group involves breaking a rather large number of symmetries of the high-symmetry phase (which was necessary in the above study to facilitate the existence of certain diffraction orders) and is not reachable through a continuous (second order) phase transition from the high-symmetry phase (i.e., the symmetry breaking distortion does not transform according to an irreducible representation of $P6_3/mmc$) rendering it energetically more costly [14, 15]. Consequently, the natural question arises whether there is a minimal inversion symmetry breaking leading to a (maximal) subgroup of the high symmetry $P6_3/mmc$ space group that would fulfill the prerequisite for hosting Néel skyrmions and be compatible with a continuous (Landau-type) phase transition [14, 15]? Such a higher symmetric non-centrosymmetric phase may exist as a metastable phase or due to inhomogeneous doping and disorder in the Fe-deficient systems, therefore not appearing in previous studies.

To address this question, this work focuses on a direct and local experimental investigation of the structural symmetry of $\text{Fe}_{2.9}\text{GeTe}_2$ bulk samples by means of electron diffraction (ED) and convergent beam electron diffraction (CBED) at room-temperature ($\text{RT} \approx 293 \text{ K}$). CBED has been widely utilized to resolve the space groups of various materials in the past since it is capable of distinguishing the presence symmetry operations such as rotational symmetry, mirror symmetry, glide plane and screw axis directly from observed symmetries in the recorded CBED patterns [16, 17], which is in contrast to x-ray or neutron diffraction, where direct read-off of inversion symmetry is hampered by Friedel’s law. Moreover, the converged electron beam employed in CBED has a diameter in the range of 10 nm, hence probing the symmetry on a local scale (in contrast to x-ray and neutron diffraction probing the average crystal symmetry over macroscopic length scales). E.g., an inspection

* subakti@um.ac.id

† a.lubk@ifw-dresden.de

of the rotational symmetries of CBED patterns recorded along the [001] zone axis immediately reveals, whether $\text{Fe}_{2.9}\text{GeTe}_2$ locally belongs to the hexagonal or trigonal system. Similarly, the existence of mirror symmetry element along c-direction of both crystal systems can be verified from CBED patterns recorded from a [uv0] zone axis.

II. CONVERGENT BEAM AND SELECTED AREAL ELECTRON DIFFRACTION

Electron diffraction experiments, employing two different illumination modes in the TEM, have been carried out to probe the symmetry of $\text{Fe}_{2.9}\text{GeTe}_2$. All experiments have been carried out at a FEI Titan3 80-300 TEM, equipped with both probe and imaging aberration correction, at 300 kV acceleration voltage.

A. Specimen Preparation

Single crystals of Fe-deficient $\text{Fe}_{2.9}\text{GeTe}_2$ have been acquired from HQ graphene, Inc. as in Ref. [8]. Subsequently, thin TEM lamella (of zone axis orientation [001] and [210]) of approximately 80 nm (for CBED) and 40 nm (for high-resolution TEM) have been cut via focused Ga⁺ ion beam milling (employing ThermoFisher Helios 5 CX FIB) using a C and Pt protection layer. After liftout of the lamella, a low-energy ion beam of 5 kV has been used for final polishing in order to remove surface damaged region.

B. SAED and CBED

The determination of crystal symmetries by electron diffraction techniques has been carried out by employing both parallel illumination electron diffraction (i.e., selected area electron diffraction – SAED) as well as convergent illumination (CBED). We used the former to determine the Bravais lattice of $\text{Fe}_{2.9}\text{GeTe}_2$, where the centering and the presence of the screw axis 6_3 is read off from systematic absences of reflections.

To uniquely characterize the point group symmetries of $\text{Fe}_{2.9}\text{GeTe}_2$, CBED patterns have been recorded along a sufficient set of zone axis orientations. For hexagonal (e.g., $P6_3/mmc$) and trigonal (e.g., $P3m1$), these zone axis orientations are [001] and [uv0], where the latter orientation probes the existence of mirror symmetry perpendicular to the c-direction. Hence, the CBED measurements clarify directly, whether the crystal belongs to the hexagonal or trigonal system, with mirror symmetry along c-direction or not. We furthermore reiterate that CBED is a local probe, i.e., the diameter of the illumination spot of the convergent electron beam in the sample plane is of the order of nanometers.

III. RESULTS

A. SAED

Fig. 1 shows SAED patterns of $\text{Fe}_{2.9}\text{GeTe}_2$ at room temperature recorded along [001] (Fig. 1a) and [210] (Fig. 1b) electron beam incidences. All the reflection spots could be indexed with a hexagonal Bravais lattice with lattice constants $a \sim 3.5 \text{ \AA}$ and $c \sim 16.2 \text{ \AA}$, notably including systematic absences ($00l=\text{odd}$) that are consistent with the presence of a screw axis 6_3 . This is further justified by high resolution TEM (HRTEM) recorded along [210] crystal plane, which shows a periodicity along c-axis of $\sim 8.1 \text{ \AA}$, corresponding to the [002] lattice plane distance (Fig. 2).

B. CBED

To determine whether $\text{Fe}_{2.9}\text{GeTe}_2$ belongs to either trigonal or hexagonal system and whether structural inversion symmetry breaking occurs, we acquired CBED patterns along the [001] (Fig. 3) and [210] (Fig. 4) zone axis. Here, the CBED pattern along [001] particularly reveals the rotational symmetry distinguishing hexagonal and trigonal system. Indeed, the position and the intensity distribution of zero order Laue zone (ZOLZ) disks (Fig. 3b) exhibit 6-fold rotational symmetry (indicated by six arrows along the circle) and two mirror symmetries (indicated by dashed lines) corresponding to a CBED diffraction group symmetry of $6mm$ (small deviations to the symmetries are attributed to small zone-axis misalignments). Besides the ZOLZ reflections, higher order Laue-zone (HOLZ) reflections appear as a ring surrounding the ZOLZ reflections (Fig. 3a). The symmetry of $6mm$ was also observed in position and intensity distribution of HOLZ reflections. Therefore, symmetry of the whole CBED pattern depicted in Fig. 3 is $6mm$.

Fig. 4a shows the whole CBED pattern of $\text{Fe}_{2.9}\text{GeTe}_2$ at room temperature recorded along [210] crystal plane. The symmetry of the whole pattern depicted in Fig. 4a appears to be m (vertical mirror plane indicated by red line) or even $2mm$ (i.e., with an additional horizontal mirror plane). A closer inspection of the ZOLZ CBED pattern Fig. 4b reveals subtle differences in the intensity distribution within the CBED discs (e.g., white arrows) that indicate the absence of 2-fold rotational symmetry and vertical mirror symmetry. The remaining vertical mirror plane symmetry is the CBED diffraction group of $6mm$ PG in [210] orientation (see coincidence tables [19]). The presence of the vertical mirror plane is additionally verified by CBED simulations employing the Dr. Probe software [20]. For the simulations 300 kV acceleration voltage and a convergence angle of 2 mrad similar to the experiment has been used. The crystal structure used in the simulations was derived from the high-symmetry phase by shifting the atoms along c-direction in accordance with the published $P3m1$ phase 8, thereby break-

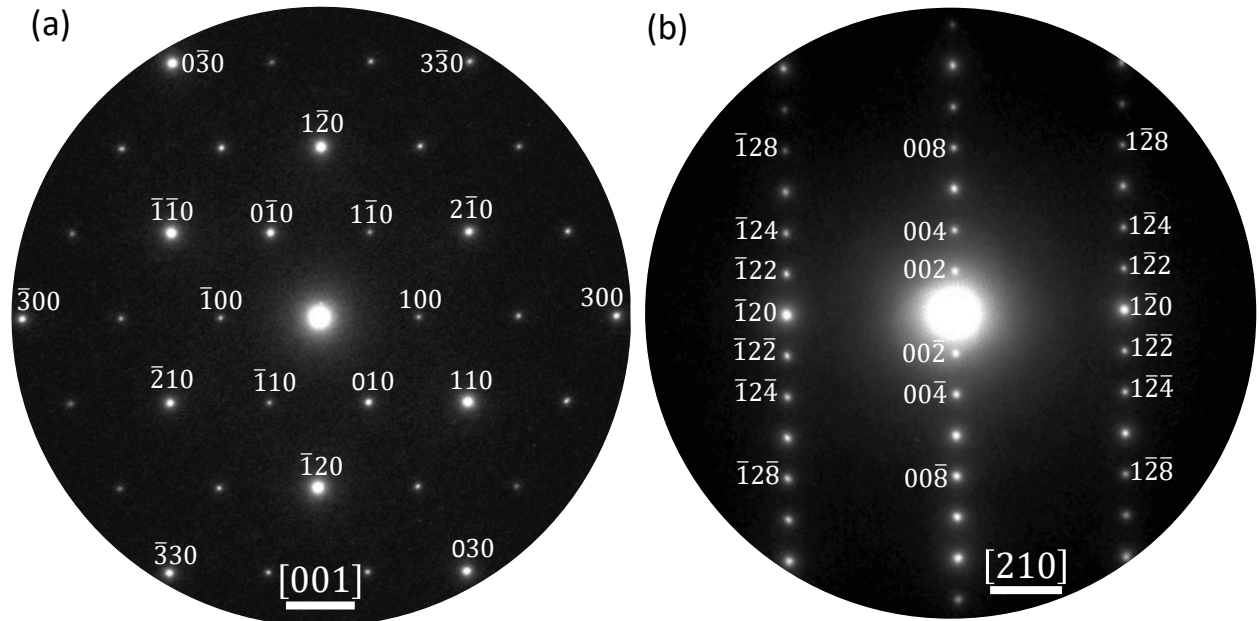


FIG. 1. Electron diffraction patterns along: (a) $[001]$ zone axis and (b) $[210]$ zone axis indexed by using hexagonal Bravais lattice (scale bar is 2 nm^{-1}) [18].

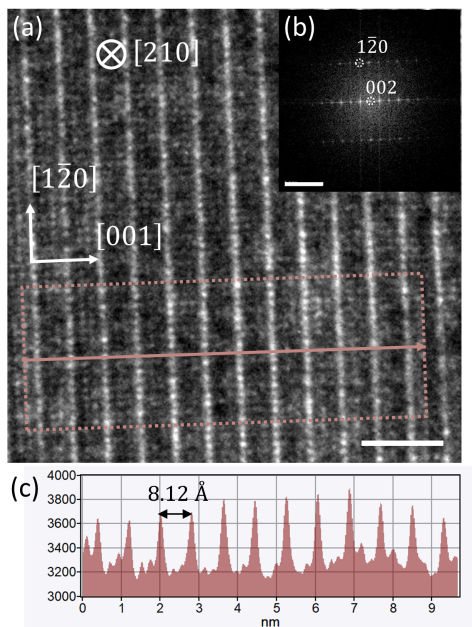


FIG. 2. High-resolution TEM (HRTEM) of $\text{Fe}_{2.9}\text{GeTe}_2$. (a) HRTEM image in $[210]$ orientation showing the pronounced (002) lattice plane along the c -axis. The scale bar is 2 nm . (b) Fourier transform of (a) verifying the (210) zone axis orientation. The scale bar is 5 nm^{-1} . (c) Line profile along the line scan indicated in (a) from revealing 8.12 \AA spacing of the (002) lattice plane.

ing the mirror symmetry along c . At a sample thickness of approximately 63 nm , a simulated CBED pattern in good agreement in contrast and symmetry with the experiment is obtained (Fig. 5b). For comparison, we also show a simulated CBED pattern of the high-symmetry $P6_3/mmc$ parent compound [18], exhibiting $2mm$ CBED symmetry (Fig. 5a and coincidence tables [19]).

The CBED patterns obtained at $[001]$ and $[210]$ electron beam incidence reveal diffraction group symmetries consistent with $6mm$ and m , respectively. Thus, the point group of $\text{Fe}_{3-x}\text{GeTe}_2$ at room temperature can be fixed to $6mm$ upon inspection of coincidence tables [19]. That also entails that the Bravais lattice is hexagonal as previously determined by SAED. To identify the corresponding space group symmetry, we first note the presence of the 6_3 screw axis, determined from systematic absences in the SAED (Fig. 1b). The presence of the 6_3 screw axis narrows the possible choice of space groups pertaining to the $6mm$ point group to either $P6_3cm$ (185) or $P6_3mc$ (186), with the latter being the natural choice considering high-symmetry space group $P6_3/mmc$ of the parent compound Fe_3GeTe_2 . Indeed, $P6_3mc$ derives from $P6_3/mmc$ by removing the mirror plane perpendicular to the rotational symmetry axis, i.e. is a maximal subgroup with index 2 of $P6_3/mmc$. Moreover, this subgroup is reachable from $P6_3/mmc$ by a continuous phase transition, i.e., at minimal energy cost [15]. Therefore, the local space group of $\text{Fe}_{2.9}\text{GeTe}_2$ at room temperature can be identified with $P6_3mc$ (No.186).

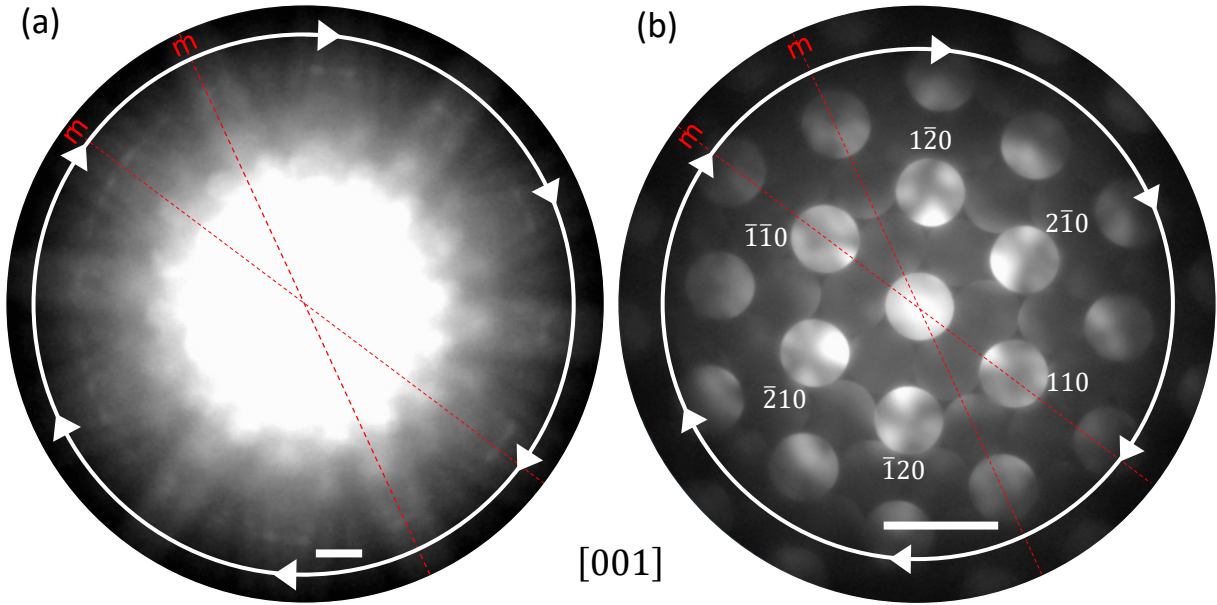


FIG. 3. CBED patterns $\text{Fe}_{2.9}\text{GeTe}_2$ along $[001]$ zone axis: (a) whole pattern CBED and (b) bright field pattern CBED (scale bar is 5 nm^{-1}).

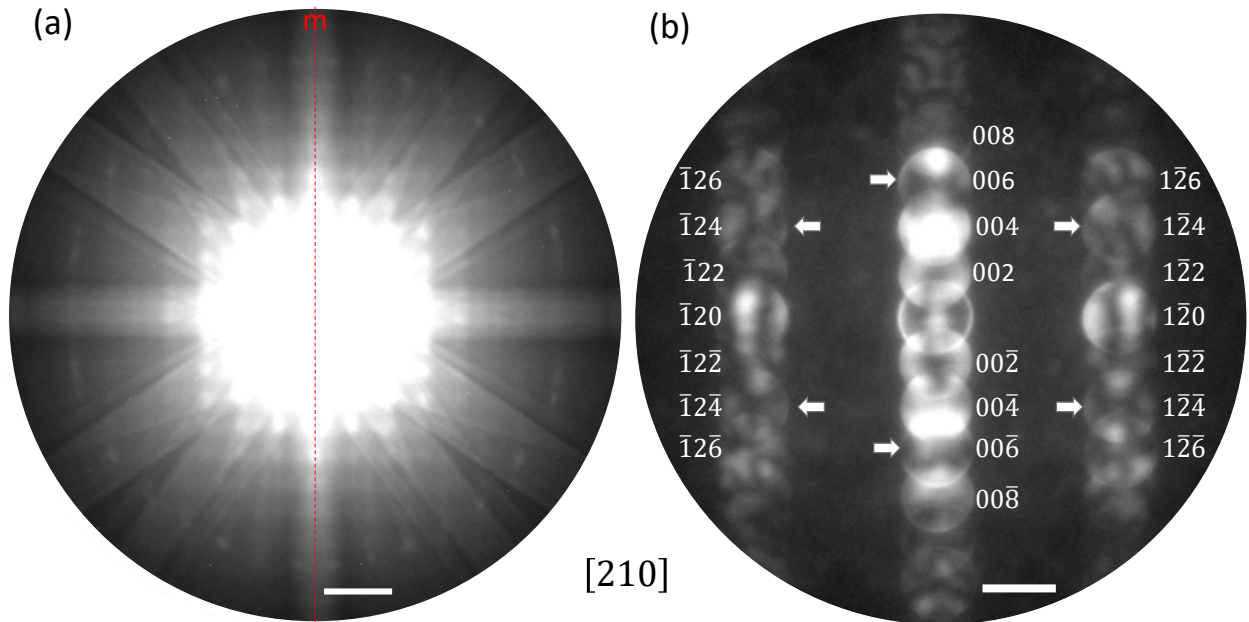


FIG. 4. CBED pattern along $[210]$ of $\text{Fe}_{2.9}\text{GeTe}_2$: (a) Whole CBED pattern suggesting m projection symmetry (scale bar is 10 nm^{-1}), (b) Bright field CBED pattern suggesting absence of symmetry (scale bar is 2 nm^{-1}).

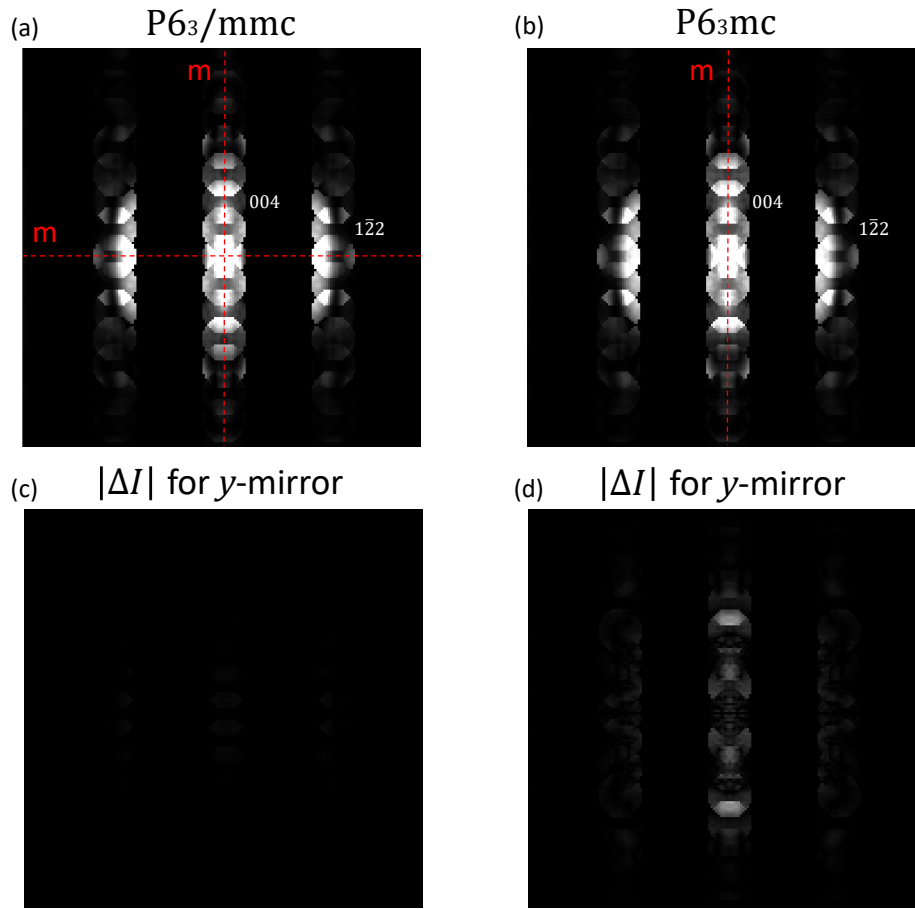


FIG. 5. CBED simulations for $[210]$ zone axis with thickness of 63 nm. Y -mirror images represent $|\Delta I| = |I - I_0|$ where I is an intensity of mirrored image.

IV. CONCLUSION

Using a combination of SAED and CBED, we determined the point group and space group symmetry of $\text{Fe}_{3-x}\text{GeTe}_2$ at room temperature to be $6mm$ and $P6_3mc$ (186), respectively. The unit cell dimensions are similar to the previously reported $P3m1$ (156) and the high-symmetry parent compound Fe_3GeTe_2 with space group $P6_3/mmc$ (194). In contrast to $P3m1$, $P6_3mc$ is reachable from the parent compound $P6_3/mmc$ through a continuous structural phase transition. Similar to $P3m1$, the absence of centrosymmetry in the $P6_3mc$ phase would support the formation of Néel skyrmion and bubbles in $\text{Fe}_{3-x}\text{GeTe}_2$ as revealed in previous studies. As the three

space groups - $P6_3/mmc$, $P6_3mc$ and $P3m1$ - form a chain of subgroups, our study indicates a scenario, where Fe deficiency leads to sequential removal of symmetries, with the mirror symmetry perpendicular to the c axis being broken first and the screw and glide plane symmetry second. Future studies may reveal the precise positions of Fe-cation deficiency clarifying this symmetry breaking mechanism.

V. ACKNOWLEDGEMENTS

This work was supported by the Deutsche Forschungsgemeinschaft through SFB 1415, project-id 417590517. This work also received support from the Deutsche Forschungsgemeinschaft DFG through the SFB 1143, project-id 24731007.

[1] H. Zhang, Y. Zhang, Z. Hou, M. Qin, X. Gao, and J. Liu, Magnetic skyrmions: materials, manipulation, detection, and applications in spintronic devices, *Materials Futures* **2**, 032201 (2023).

[2] H. L. Zhuang, P. R. C. Kent, and R. G. Hennig, Strong anisotropy and magnetostriction in the two-dimensional stoner ferromagnet Fe_3GeTe_2 , *Phys. Rev. B* **93**, 134407 (2016).

- [3] A. F. May, S. Calder, C. Cantoni, H. Cao, and M. A. McGuire, Magnetic structure and phase stability of the van der waals bonded ferromagnet $\text{Fe}_{3-x}\text{GeTe}_2$, *Phys. Rev. B* **93**, 014411 (2016).
- [4] A. Milosavljević, A. Šolajić, S. Djurdjić Mijin, J. Pešić, B. Višić, Y. Liu, C. Petrovic, N. Lazarević, and Z. V. Popović, Lattice dynamics and phase transitions in $\text{Fe}_{3-x}\text{GeTe}_2$, *Phys. Rev. B* **99**, 214304 (2019).
- [5] P. Yang, R. Liu, Z. Yuan, and Y. Liu, Magnetic damping anisotropy in the two-dimensional van der waals material Fe_3GeTe_2 from first principles, *Phys. Rev. B* **106**, 134409 (2022).
- [6] H.-J. Deiseroth, K. Aleksandrov, C. Reiner, L. Kienle, and R. K. Kremer, Fe_3GeTe_2 and Ni_3GeTe_2 – two new layered transition-metal compounds: Crystal structures, hrtm investigations, and magnetic and electrical properties, *European Journal of Inorganic Chemistry* **2006**, 1561 (2006).
- [7] B. Liu, S. Liu, L. Yang, Z. Chen, E. Zhang, Z. Li, J. Wu, X. Ruan, F. Xiu, W. Liu, L. He, R. Zhang, and Y. Xu, Light-tunable ferromagnetism in atomically thin Fe_3GeTe_2 driven by femtosecond laser pulse, *Phys. Rev. Lett.* **125**, 267205 (2020).
- [8] A. Chakraborty, A. K. Srivastava, A. K. Sharma, A. K. Gopi, K. Mohseni, A. Ernst, H. Deniz, B. K. Hazra, S. Das, P. Sessi, I. Kostanovskiy, T. Ma, H. L. Meyerheim, and S. S. P. Parkin, Magnetic skyrmions in a thickness tunable 2d ferromagnet from a defect driven dzyaloshinskii–moriya interaction, *Advanced Materials* **34**, 2108637 (2022).
- [9] N. León-Brito, E. D. Bauer, F. Ronning, J. D. Thompson, and R. Movshovich, Magnetic microstructure and magnetic properties of uniaxial itinerant ferromagnet Fe_3GeTe_2 , *Journal of Applied Physics* **120**, 083903 (2016).
- [10] J. M. J. Lopes, D. Czubak, E. Zallo, A. I. Figueroa, C. Guillemand, M. Valvidares, J. Rubio-Zuazo, J. López-Sánchez, S. O. Valenzuela, M. Hanke, and M. Ramsteiner, Large-area van der waals epitaxy and magnetic characterization of Fe_3GeTe_2 films on graphene, *2D Materials* **8**, 041001 (2021).
- [11] J. Eom, I. H. Lee, J. Y. Kee, M. Cho, J. Seo, H. Suh, H.-J. Choi, Y. Sim, S. Chen, H. J. Chang, S.-H. Baek, C. Petrovic, H. Ryu, C. Jang, Y. D. Kim, C.-H. Yang, M.-J. Seong, J. H. Lee, S. Y. Park, and J. W. Choi, Voltage control of magnetism in $\text{Fe}_{3-x}\text{GeTe}_2/\text{In}_2\text{Se}_3$ van der waals ferromagnetic/ferroelectric heterostructures, *Nature Communications* **14**, 5605 (2023).
- [12] C. Xu, X. Li, P. Chen, Y. Zhang, H. Xiang, and L. Bellaiche, Assembling diverse skyrmionic phases in Fe_3GeTe_2 monolayers, *Advanced Materials* **34**, 2107779 (2022).
- [13] M. T. Birch, L. Powalla, S. Wintz, O. Hovorka, K. Litzius, J. C. Loudon, L. A. Turnbull, V. Nehruji, K. Son, C. Bubeck, T. G. Rauch, M. Weigand, E. Goering, M. Burghard, and G. Schütz, History-dependent domain and skyrmion formation in 2d van der waals magnet Fe_3GeTe_2 , *Nature Communications* **13**, 3035 (2022).
- [14] H. F. Franzen, C. Haas, and F. Jelinek, Phase transitions between nias- and mnp-type phases, *Phys. Rev. B* **10**, 1248 (1974).
- [15] J. M. Perez-Mato, J. L. Manes, M. J. Tello, and F. J. Zuniga, Structural phase transitions in crystals with $P6_3/mmc$ symmetry, *Journal of Physics C: Solid State Physics* **14**, 1121 (1981).
- [16] M. Tanaka and K. Tsuda, Convergent-beam electron diffraction, *J. Electron Microsc. (Tokyo)* **60**, S245 (2011).
- [17] J. Morniroli, G. Ji, and D. Jacob, A systematic method to identify the space group from ped and cbed patterns part i - theory, *Ultramicroscopy* **121**, 42 (2012).
- [18] V. Y. Verchenko, A. A. Tsirlin, A. V. Sobolev, I. A. Presniakov, and A. V. Shevelkov, Ferromagnetic order, strong magnetocrystalline anisotropy, and magnetocaloric effect in the layered telluride $\text{Fe}_{3.5}\text{GeTe}_2$, *Inorganic Chemistry* **54**, 8598 (2015).
- [19] B. F. Buxton, J. A. Eades, J. W. Steeds, G. M. Rackham, and F. C. Frank, The symmetry of electron diffraction zone axis patterns, *Philos. Trans. R. Soc. London. Ser. A, Math. Phys. Sci.* **281**, 171 (1976).
- [20] J. Barthel, Dr. probe: A software for high-resolution stem image simulation, *Ultramicroscopy* **193**, 1 (2018).